Spectrochimica Acta Part A 75 (2010) 54–60

Contents lists available at ScienceDirect

Spectrochimica Acta Part A: Molecular and Biomolecular Spectroscopy

journal homepage: www.elsevier.com/locate/saa

Synthesis, spectroscopy, and quantum-chemical calculations on 1-substituted phenyl-3,5-diphenylformazans

Habibe Tezcan[a,*], Nesrin Tokay[b]

[a] Gazi University, Education Faculty, Department of Chemistry, Teknikokullar 06500, Ankara, Turkey
[b] Hacettepe University, Faculty of Science, Department of Chemistry, 06532 Beytepe, Ankara, Turkey

ARTICLE INFO

Article history:
Received 15 January 2009
Received in revised form 3 August 2009
Accepted 24 September 2009

Keywords:
Formazans
IR
UV–vis spectroscopy
Substituent effect
Density-functional theory
Time-dependent density-functional theory

ABSTRACT

In this study 1-substituted phenyl-3,5-diphenylformazans were synthesized from benzaldehyde-N-phenylhydrazone and appropriate phenyldiazonium salts having CH_3, Br, and Cl at the *o*-, *m*-, and *p*-positions of 1-phenyl ring. Their structures were determined by infrared and ultraviolet–visible spectra. Bathochromic effect in accordance with the electron-donating effect of CH_3, Br, and Cl group and its magnitude were dependent upon type and position of substituent on the ring. The ground-state geometries and absorption wavelengths for 1-phenyl substituted formazans were studied with density functional theory and time-dependent density functional theory. The calculations were carried out by using PBE1PBE functional with 6-311G(2d,2p) basis set for λ_{max} of the UV–vis spectra for the studied formazans. A good agreement was obtained between the experimental and computed values.

1. Introduction

There have been numerous formazans synthesized and their structural, spectral features, and reaction mechanisms of formation were elucidated [1–6]. Because there are important using fields of formazans, for example: analytical reagents, trace element determination, biochemical markers for redox processes, photo- and thermochromic materials. Formazans form tetrazolium salt when they are oxidized [7]. Tetrazolium salts are reduced back to formazans by enzymes in cell and stain tissue. That is why tetrazolium/formazan system is classified as a marker of vitality [8], and used for screening of anti cancer drugs, determination of activity on tumor cell, and of sperm viability [9–11]. These features cause an increasing interest especially in electrochemical and spectral properties of tetrazolium/formazan systems. For these reasons, in our previous work we investigated electrochemical behaviors of some formazans [12]. Moreover, we carried out semiempirical calculation on some formazans [13].

As a predictive tool for electronic structural properties, molecular modelization techniques allow a solution for the interpretation of experimental data. For the calculation of electronic structures of large molecules, the most widely used method is density functional theory (DFT) [14]. It has been known that the absorption spectrum is related to the molecular structure and a relationship between the absorption maximum and the structure mostly be desired. In order to achieve this, experimental spectrum can be compared with calculated one. The extension of DFT to excited states is known as the time-dependent density functional theory (TD-DFT) method and used to describe optical and spectroscopic properties of medium and large molecules [15]. A limited numbers of DFT and TD-DFT investigations have been carried out on formazans [16,17].

In this study, formazans with various substituents (CH_3, Br, and Cl) on 1-phenyl ring were synthesized (Scheme 1). Their structures were elucidated by using elemental analysis, IR, and UV–visible spectra. The effect of substituents was also determined by considering λ_{max} shift for both experimental and theoretical values. The main aim was to carry out a systematic theoretical study and to compare experimental and calculated results. The optimized structural parameters, oscillator strengths and the maximum absorption peaks (λ_{max}) were investigated by using DFT and TD-DFT methods.

2. Experimental

2.1. General

The infrared (IR) spectra were recorded on a UNICAM SP-1025 spectrophotometer between 4000 and 400 cm^{-1} in KBr pellets. The ultraviolet–visible (UV–vis) spectra were obtained with PerkinElmer 550 spectrophotometer using 1 cm quartz cell, in 10^{-4} M CH_3OH in the range of 200–650 nm. The elemental analysis studies were carried out by LECO-CHNS-932 elemental analyzer. All chemicals were purchased from Merck, Fluka Sigma–Aldrich.

* Corresponding author. Tel.: +90 312 202 82 59; fax: +90 312 222 70 37.
E-mail address: habibe@gazi.edu.tr (H. Tezcan).

1386-1425/$ – see front matter © 2009 Elsevier B.V. All rights reserved.
doi:10.1016/j.saa.2009.09.034

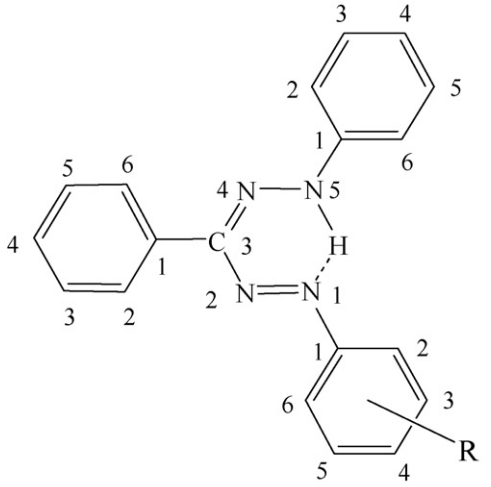

1. R: H
2. R: *o*-CH_3 **5**. R: *o*-Br **8**. R: *o*-Cl
3. R: *m*-CH_3 **6**. R: *m*-Br **9**. R: *m*-Cl
4. R: *p*-CH_3 **7**. R: *p*-Br **10**. R: *p*-Cl

Scheme 1. The structure of the formazan derivatives.

Organic solvents were used without further purification, and deionized water (Millipore, Milli-Q) was used for synthesis.

2.2. Synthesis of formazans

The synthesis was carried out following the route suggested by Refs. [1–3]. Benzaldehyde–phenylhydrazone was prepared by adding phenylhydrazine solution (in CH_3OH) into benzaldehyde solution (in CH_3OH) at the 25 °C, and pH 5–6. The resulting hydrazone was filtered and recrystallized from solution by using methanol as solvent and washed with methanol and water respectively. The product was dissolved in CH_3OH. The solution was added into basic buffer solution of 2.50 g NaOH and 3.50 g CH_3COONa in CH_3OH. On the other hand, the diazonium salts were prepared by known procedure from aniline or substituted anilines. The formazans were obtained by coupling diazonium salts with benzaldehyde–phenylhydrazones in pH 10–12. Each compound was recrystallized by using methanol as solvent. All formazans were synthesized by the same procedure. Here we will only give experimental and spectral data.

2.2.1. 1,3,5-Triphenylformazan [***TPF(1)***]

Cheery-red; yield 78%; m.p. 172–173 °C; lit: 170–173 °C. Anal. calc. for $C_{19}H_{16}N_4$: C; 76.00, H; 5.33, N; 18.66. Found: C; 76.04, H; 5.31, N; 18.62.

2.2.2. 1-(o-Methyl)-3,5-diphenylformazan (***2***)

Bright red color; yield 78%; m.p 152–154 °C; lit: 154 °C. Anal. calc. for $C_{20}H_{18}N_4$: C; 76.43, H; 5.73, N; 17.83. Found: C; 76.23, H; 5.62, N; 17.78.

*1-(m-Methyl)-3,5-diphenylformazan (**3**)*: Bright red color; yield 73%; m.p. 150 °C.

*1-(p-Methyl)-3,5-diphenylformazan (**4**)*: Bright red color; yield 78%; m.p.154; lit: 155 °C.

2.2.3. 1-(o-Bromophenyl)-3,5-diphenylformazan (***5***)

Dark red color; yield 73%; m.p 149 °C. Anal. Calc. for $C_{19}H_{15}N_4Br$: C; 60.15, H; 3.96, N; 14.77. Found: C; 59.85, H; 3.92, N; 14.62.

*1-(m-Bromophenyl)-3,5-diphenylformazan (**6**)*: Dark red color; yield 70%; m.p. 120–122 °C.

*1-(p-Bromophenyl)-3,5-diphenylformazan (**7**)*: Red color; yield 74%; m.p. 189 °C; lit: 191 °C.

2.2.4. 1-(o-Chlorophenyl)-3,5-diphenylformazan (***8***)

Dark red color; yield 76%; m.p 143 °C. Anal. calc. for $C_{19}H_{15}N_4Cl$: C; 68.26, H; 4.49, N; 16.76. Found: C; 68.12, H; 4.35, N; 17.01.

*1-(m-Chlorophenyl)-3,5-diphenylformazan (**9**)*: Red color; yield 74%; m.p 158 °C.

*1-(p-chlorophenyl)-3,5-diphenylformazan (**10**)*: Bright red color; yield 72%; m.p. 119 °C; lit: 117 °C.

2.3. Computational method

All calculations were carried out with the Gaussian 03 package program [18]. Quantum-chemical calculations of **TPF** have been performed using Becke's three parameter exchange function (B3) with Lee–Yang–Parr correlation function (LYP), and Perdew, Burke, and Ernzerhof (PBE) functionals with several basis sets: 6-31, 6-31G(d), 6-31G(d,p), 6-311G(d,p), 6-311G(2d,2p), 6-31+G(d,p), and 6-311++G(d,p) [19–21]. In order to decide which functional and basis set are suitable, the experimental structural data of **TPF** is needed. But there is no any experimental structural data of **TPF**. It is possible to compare of experimental and calculated λ_{max} of **TPF**. The comparison of experimental and calculated λ_{max} of **TPF** revealed that the combinations PBE1PBE functional with 6-31G(d), 6-31G(d,p), 6-311G(d,p), and 6-311G(2d,2p) basis sets were suitable. So, following quantum-chemical calculations were performed by using these combinations of functional and basis sets.

Geometry optimizations of formazans in gas phase were carried out at DFT level of theory using PBE1PBE with four basis sets without any symmetry restrictions. Following each optimization, vibrational spectrum has been determined to check that all vibrational frequencies are real.

Then, the vertical excitation energy calculations were performed by using TD-DFT method with the same level of theory selected for geometry optimization. It is known that the maximum absorption wavelengths (λ_{max}) in the UV–vis spectrum correspond to the vertical excitation energies. For TD-DFT calculations, the Polarizable Continuum Model (PCM) was used to take care of the solvent effects [22].

3. Results and discussion

3.1. Synthesis of formazans

There are three distinctive routes proposed to synthesize formazans in literature [1]. In this study the formazans were synthesized by coupling of hydrazones with diazonium cations in basic media at −5 to 0 °C. The best yield was obtained with the NaOH + CH_3COONa buffer solution (pH 10–12). The hydrazone was synthesized by the condensation reaction of benzaldehyde and phenylhydrazine at pH 5–6. The possible formation mechanism of the studied formazans was given in Scheme 2.

The reason to prefer this route is that the starting materials are easily found in all laboratories. It has also the advantage of synthesizing symmetrical and asymmetrical formazans [1–3]. We tried to increase the yield and to provide a cheap method to synthesize formazans for dying and analytic applications and medical purpose.

3.2. Spectral behavior

The IR and UV–vis spectral data of 1-(substituted phenyl)-3,5-diphenylformazans are listed in Tables 1 and 2 respectively. The structure in Scheme 1 was supported by elemental analysis, IR, UV–visible spectra. It was observed vibration peaks at 3100 cm^{-1} for Arom. C–C, at 1610 cm^{-1} for Arom. C=C,

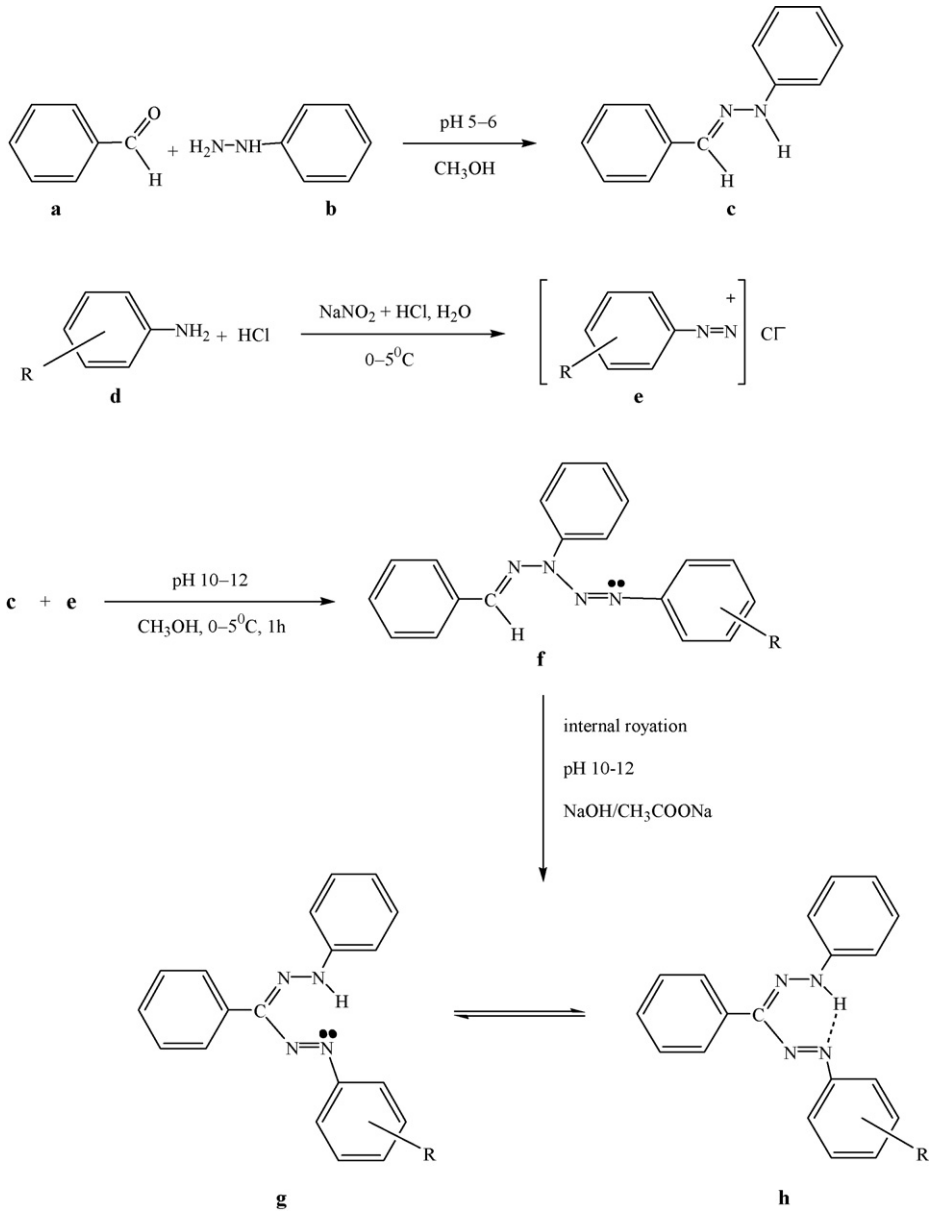

Scheme 2. The formation mechanism of formazans.

at 1450–1455 cm^{-1} for N=N, at 1270–1365 cm^{-1} for C–N1, at 1200 cm^{-1} for C–N4, at 1035–1190 cm^{-1} for N1–N2, and stretching peaks at 1505–1530 cm^{-1} for C=N.

When 1-phenyl ring is substituted with bulky groups such as Cl, Br, 5-phenyl ring is repulsed by these groups. C=N stretching band appears at 1565–1551 cm^{-1} for non-chelate structures and at 1510–1500 cm^{-1} for chelate structures [2,23,24]. **1–4** must be in chelate structure since the C=N stretching band appeared at 1510–1500 cm^{-1}. However, the C=N stretching bands of Cl, Br-substituted formazans (**5–10)** occurred at 1520–1530 cm^{-1}. These values indicated that chelate and non-chelate structures were in equilibrium and the amount of non-chelate structures was less than that of chelate structures (Scheme 3). Besides the peaks at the fingerprint range (825–910 cm^{-1}) are the proof of formazans struc-

Table 1
IR spectral data of formazans **1-10**, (KBr, cm^{-1}).

Compound	Arom. C–H	Arom. C=C–	C=N	N=N	C–N^1	C–N^4	N_1–N_2 valance	CNNC skeleton	Arom. C–H plane out
1	–	1610	1505	1455	1365	1200	1190,1160,1035	931–905	755,705,650
2	3100	1610	1505	1455	1365	1190–1120	1090,1060,1035	951–840	770,705,650
3	3100	1610	1505	1455	1365	1200–1150	1090,1060,1035	930–840	770,705,650
4	–	1610	1505	1455	1365	1200–1080	1110,1160,1035	930–840	770,705,650
5	–	1610	1520	1455	1270	1195–1170	1090,1060,1035	930–825	770,705,650
6	3100	1610	1520	1455	1370	1195–1170	1090,1060,1035	930–840	770,705,650
7	3100	1605	1500	1450	1160	1200–1180	1180,1155,1080	935–840	780,705,650
8	3095	1610	1525	1450	1365	1190–1160	1080,1050,1030	925–825	755,700,645
9	3100	1610	1535	1455	1370	1200	1085,1060,1035	910,895,840	785,810,650
10	–	1610	1530	1455	1370	1200	1100,1060,1035	930,910,850	780,750,650

Table 2
Experimental and calculated λ_{max} (in CH_3OH) of studied compounds.

Compound	Experimental values			PBE1PBE[a]							
	λ_{max} (nm) – (Abs)	Shift max[b]	σ	6-31g(d)		6-31g(d,p)		6-311g(d,p)		6-311g(2d,2p)	
				λ_{max}	f	λ_{max}	f	λ_{max}	f	λ_{max}	f
1	482.0 – (0.630)		–	486.0	0.5420	486.2	0.5408	486.1	0.5490	**484.7**	0.5397
2a	489.0 – (0.623)	−7.0	–	490.1	0.5162	490.3	0.5150	490.1	0.5224	**488.9**	0.5250
2b				479.8	0.5355	480.0	0.5345	480.0	0.5400	478.4	0.5425
3a	488.0 – (0.402)	−6.0	−0.07	486.5	0.5380	486.4	0.5370	485.6	0.5460	484.0	0.5504
3b				488.2	0.5541	486.3	0.5582	485.9	0.5678	**484.5**	0.5724
4	487.0 – (0.423)	−5.0	−0.17	488.2	0.5839	488.1	0.5838	487.7	0.5957	**485.7**	0.6027
5a	487.0 – (0.987)	−5.0	–	501.6	0.4678	500.8	0.4681	497.7	0.4803	**496.2**	0.4816
5b				475.3	0.4902	475.6	0.4891	473.5	0.4759	471.7	0.4725
6a	487.0 – (0.852)	−5.0	0.39	497.7	0.5557	498.1	0.5528	494.7	0.5707	492.1	0.5422
6b				495.5	0.5215	494.3	0.5258	493.3	0.5387	**493.4**	0.5766
7	489.0 – (1.167)	−7.0	0.23	498.9	0.6064	499.0	0.6048	497.8	0.6093	**496.5**	0.6142
8a	486.0 – (0.418)	−4.0	–	499.4	0.4902	499.0	0.4870	498.6	0.4959	**497.3**	0.4989
8b				475.9	0.4785	476.2	0.4775	475.1	0.4801	473.3	0.4758
9a	486.0 – (0.650)	−4.0	0.373	494.0	0.5284	495.9	0.5211	493.7	0.5384	492.2	0.5425
9b				497.0	0.5438	494.4	0.5500	494.3	0.5611	**492.8**	0.5670
10	489.0 – (0.630)	−7.0	0.22	496.5	0.5865	496.5	0.5847	495.7	0.5964	**494.4**	0.6053

[a] The bold values are considered for comparison.
[b] $\Delta\lambda_{max} = \lambda_{max}(\mathbf{TPF}) - \lambda_{max}$(substituted formazans).

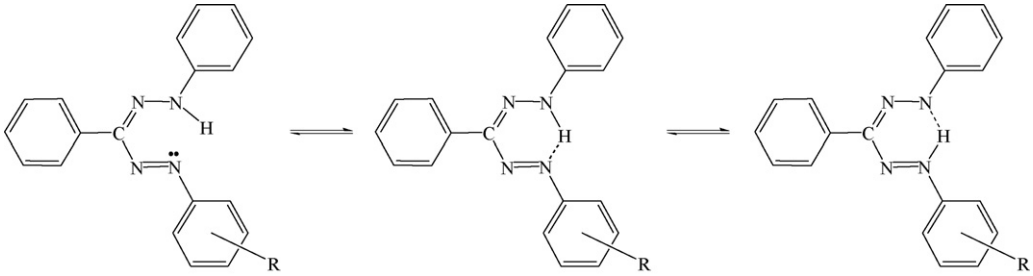

Scheme 3. Molecular chelation and symmetry of 1-substituted phenyl-3,5-diphenylformazans.

tures [2,23]. Also IR and UV–vis data and appearance of spectra are the characteristics of formazan skeleton.

As seen from Table 2, characteristic absorption peak of 1,3,5-triphenylformazan shows a maximum at 482.0 nm, while *o*-, *m*-, and *p*-CH_3 substituted formazans gave absorption maxima at 489.0 nm, 488.0 nm, and 487.0 nm respectively. Bathochromic shift was observed in all positions and shift values were in the order of *o* > *m* > *p*-positions. The gradual decrease in the shift values from *o*- to *p*-positions can be attributed to the gradual decrease in the inductive electron-donating effect of CH_3.

In *o*-Cl and *o*-Br-substituted compounds, the λ_{max} value shifted due to the facts that their inductive electron withdrawing and resonance electron-donating effects impose an opposing effect on each other. But inductive effect is decreased for *m*-Cl and *m*-Br-substituted compounds. For this reasons, the bathochromic effects are the same for the *o*- and *m*-positions (**5** with **6**, and **8** with **9**). λ_{max} shifted 1 nm for Cl less than Br because of the difference in their electronegativity values. At *p*-position, λ_{max} shifted the for both substituents (compounds **7** and **10**) and acted as electron-donating groups due to the resonance effect. These results are shown in Fig. 1 by comparing to **TPF**. A correlation was investigated between Hammett substituent coefficients σ and absorption λ_{max} values. As seen from Fig. 2, there is a linear relation between σ and λ_{max} values.

3.3. Calculation results

3.3.1. Geometric structures

Since there is no experimental structural data of any formazan, it is impossible to decide which method is better for determination of the ground-state structures of formazans. Because of the medium size of **TPF** and its sensitivity to the methods, it was chosen to determine the best method and basis set. Buemi et al. [16] reported that there are many possible conformations of **TPF**. King and Murrin [17] found three structural minima for **TPF**. They also found that the global minimum has the *trans-syn-s-cis* (TSSC) conformation (Scheme 1). Because of being the most stable conformer, TSSC conformation of **TPF** was selected to determine the best method and basis set. Initially the optimized geometrical data of **TPF** were determined by using B3LYP and PBE1PBE functionals with several basis sets. In order to ensure it to be a true local minimum, optimized geometry was confirmed by vibrational frequency calculation at the same level of theory. Imaginary vibrational frequencies were absent in an optimized structure signifying true minimum. Then

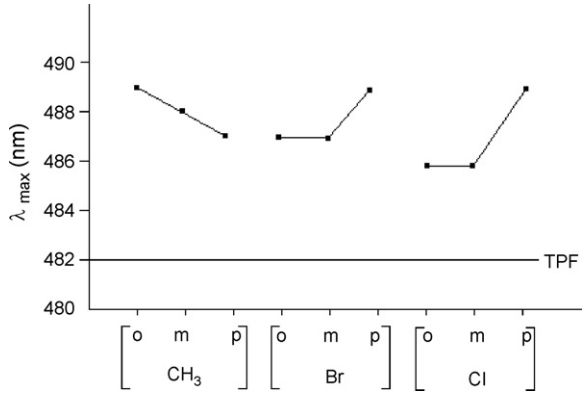

Fig. 1. Absorption λ_{max} value of the substituted formazans compared to **TPF**.

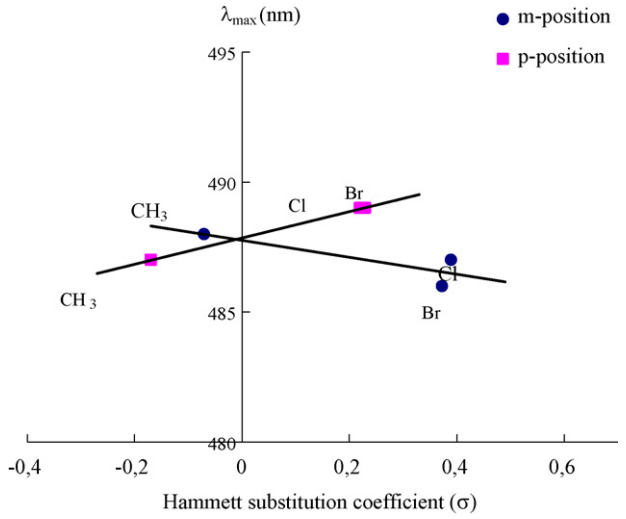

Fig. 2. λ_{max} values versus Hammett substituent coefficient (σ).

Table 3
λ_{max} (in CH_3OH) and oscillator strengths of **TPF**[a] calculated with two functionals and different basis sets.

Functional / Basis set	B3LYP		PBE1PBE	
	λ	*f*	λ	*f*
6-31G	510.3	0.4892	490.5	0.5214
6-31G(d)	504.6	0.5115	486.2	0.5408
6-31G(d,p)	504.5	0.5108	486.0	0.542
6-311G(d,p)	503.1	0.5226	486.1	0.549
6-311G(2d,2p)	501.3	0.5265	484.7	0.5528
6-31G+(d,p)	518.1	0.5133	497.8	0.5397
6-311G++(d,p)	512.2	0.5186	493.7	0.5434

[a] The experimental λ_{max} is 482.0 nm.

the UV–vis data of **TPF** were calculated with TD-DFT using the same functionals and basis sets that were used in geometry optimization. Table 3 lists the data of calculated λ_{max} for **TPF** in CH_3OH. The experimental λ_{max} value of is 482.0 nm. The calculated λ_{max} values for **TPF** are 486.2, 486.0, 486.1, and 484.7 nm for the combinations of PCM-PBE1PBE functional with 6-31G(d), 6-31G(d,p), 6-311G(d,p), and 6-311g(2d,2p) basis sets. It was concluded that the combinations of PCM-PBE1PBE functional with 6-31G(d), 6-31G(d,p), 6-311G(d,p), and 6-311g(2d,2p) basis sets provide the better results.

For geometric structure discussions, gas phase PBE1PBE/6-311G(2d,2p) results were considered. The stability of **TPF** can be explained by the conjugation within the pseudo six-membered ring (chelate) (Scheme 3). The chelate is completed by N···H bond whose length was found as 1.79 Å for **TPF** and all other studied compounds. In addition, the delocalization in the ring can be explained by considering the central C–N bond lengths. The two C–N bonds have similar bond lengths of 1.379 and 1.312 Å in **TPF**. The differences in the same bonds are very small (±0.001 and ±0.002 Å respectively) for other formazans (Table 4).

Table 4
Some selected bond lengths of studied formazans at PBE1PBE/6-311G(2d,2p) level.

Compound	H-bond	N–H bond	C–N bond	
	H···N1	N5–H	C3–N2	C3–N4
1	1.785	1.025	1.379	1.312
2a	1.793	1.025	1.379	1.311
2b	1.787	1.024	1.385	1.310
3a	1.788	1.024	1.380	1.311
3b	1.789	1.025	1.380	1.311
4	1.800	1.024	1.380	1.311
5a	1.800	1.025	1.374	1.341
5b	1.790	1.024	1.380	1.312
6a	1.788	1.025	1.377	1.313
6b	1.788	1.025	1.377	1.313
7	1.785	1.025	1.377	1.313
8a	1.783	1.026	1.374	1.315
8b	1.789	1.024	1.380	1.312
9a	1.788	1.025	1.377	1.313
9b	1.788	1.025	1.377	1.313
10	1.791	1.024	1.377	1.313

It can be seen from Scheme 1 that for substituation there are two possibilities for both *o*- and *m*-positions. At *o*-position, it is expected that C6-substituted formazans (**b**-type) are more stable than C2-substituted formazans (**a**-type). But it can be seen from Table 5 that **a**-type are more stable than **b**-type. This is explained by the increasing effect of resonance of the chelate (Section 3.2) by electron-donating substituents on C2 (**a**-type). For *m*-position there are no big differences in the heats of formation (Table 5) and other parameters (Tables 4 and 6) between C3 (**a**-type) and C5 (**b**-type) substituted formazans.

It can be seen from Table 6 that the Ph–N=N–C=N–N–Ph skeletons of all studied formazans are nearly planar because of the pseudo six-membered ring. The torsion angle N1–N2–C3–N4 is −5.40°, −7.67° and −7.02°. But there are three exceptions of the planar structure: **2b**, **5b**, and **8b** (*o*-substituted formazans). As mentioned in Section 3.2, if 1-phenyl ring is substituted with bulky groups (Cl, Br, etc.) 5-phenyl ring is repulsed by these groups. The torsion angle of the Ph-group bonded to N1 is −9.75°, −39.41° and −37.13° for **2b**, **5b**, and **8b** respectively. The phenyl group bonded to C3 atom on the skeleton of formazan is out of this plane for all studied compounds. The minimum torsion angle for this group is −15.28° (**2a**) and of the maximum 16.61° (**10**). For *o*-bromo formazan, the substituted 1-phenyl group is also out of the plane. It can be explained that the volume of bromine atom is greater than of hydrogen. Therefore the steric effect of bromine is greater than other substituents (CH_3, Cl). This is explained by repulsion between bromine with 5-phenyl group. The degrees of the torsion angles of *o*-Cl and *o*-CH_3 decrease respectively.

3.3.2. *The effect of substitution on UV–vis spectra*

Table 2 includes experimental and calculated λ_{max} values with highest oscillator strength. The PCM-TD-PBE1PBE approach was applied to determine λ_{max} of formazans in CH_3CH solution. The results which were obtained by 6-311G(2d,2p) basis set are more close to experimental data than other basis sets. For studied compounds, the minimum deviation between calculated

Table 5
Calculated heats of formation of studied formazans (in Hartree) obtained by PBE1PBE/6-311G(2d,2p) calculations.

Compound	ΔH_f	Compound	ΔH_f	Compound	ΔH_f
1	−951.73299				
2a	−991.01277	**5a**	−3524.94959	**8a**	−1411.19686
2b	−991.00828	**5b**	−3524.94077	**8b**	−1411.18839
3a	−991.01308	**6a**	−3524.95022	**9a**	−1411.19770
3b	−991.01326	**6b**	−3524.95031	**9b**	−1411.19784
4	−991.0136	**7**	−3524.95083	**10**	−1411.19838

Table 6
Selected torsion angles (°) of formazans obtained by PBE1PBE/6-311G(2d,2p) calculations.

Compound	N1–N2–C3–N4	N5–N4–C3–N2	N2–N1–C1–C6	N2–C3–C1–C2	N4–N5–C1–C2
1	−1.0	−0.3	−9.3	−15.4	−3.5
2a	1.3	−1.4	−9.0	−15.3	−3.8
2b	−5.4	2.8	−9.8	12.0	1.9
3a	1.9	−0.2	11.1	15.1	2.9
3b	2.0	−0.2	10.8	16.2	3.3
4	1.1	0.0	7.7	15.6	2.1
5a	1.7	−0.3	14.4	16.7	6.6
5b	−7.7	3.9	−39.4	6.6	0.3
6a	2.1	−0.5	10.3	17.1	2.5
6b	1.5	0.1	10.2	16.3	3.4
7	2.1	0.2	−9.8	−15.3	−3.8
8a	0.9	0.1	12.1	16.4	5.5
8b	−7.0	3.7	−37.1	7.2	0.7
9a	−0.2	0.9	8.4	16.3	3.2
9b	−1.5	−0.1	−10.0	−16.3	−3.4
10	1.8	−0.2	9.6	16.6	3.1

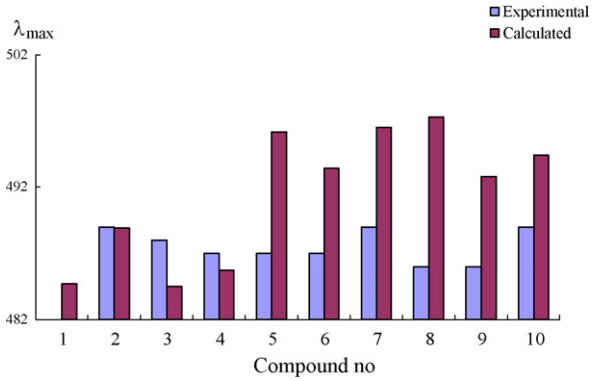

Fig. 3. The experimental and calculated λ_{max} values of studied formazans.

by PCM-TD-PBE1PBE/6-311G(2d,2p)//PBE1PBE/6-311G(2d,2p) and experimental λ_{max} is 0.1 nm for **2a**, and the maximum deviation is 11.3 nm for **8a**. As seen Fig. 3, there is a good correlation between the calculated and experimental absorption λ_{max} values of substituted formazans. In the literature, if the difference is nearly 10 nm, it can be assumed that there is a good agreement between experimental and calculated λ_{max} [25].

CH_3, Br, and Cl substituents on 1-phenyl affect the electron density on the Ph–N=N–C=N–N–Ph main skeleton. For **a**-type compounds that are *o*-substituted formazans, the conjugated part becomes larger because of the joining of substituents to the conjugation on C2. The greater conjugated part causes the lowering of the energy difference between HOMO and LUMO, and makes λ_{max} longer relative to that of unsubstituted dye, **TPF** (Table 2 and Scheme 1) (bathocromic effect). The formazans that have substituents at *m*-position (on C5) have shorter λ_{max}. This is explained by the electron-donating effect of CH_3 at *m*-position that is the hyperconjugation or it is known as "non-bonding resonance". Cl and Br at *m*-position participate to the resonance by their lone-pair

Table 7
Frontier orbital energies (eV) of studied formazans at PCM-TD-PBE1PBE/6-311G(2d,2p)//PBE1PBE/6-311G(2d,2p) level.[a]

Frontier orbitals	Compound															
	1	**2a**	**2b**	**3a**	**3b**	**4**	**5a**	**5b**	**6a**	**6b**	**7**	**8a**	**8b**	**9a**	**9b**	**10**
HOMO	−5.69	−5.70	−5.65	−5.68	−5.68	−5.65	−5.77	−5.76	−5.76	−5.76	−5.72	−5.76	−5.76	−5.76	−5.76	−5.72
LUMO	−2.65	−2.67	−2.57	−2.64	−2.64	−2.61	−2.78	−2.66	−2.77	−2.77	−2.75	−2.79	−2.66	−2.77	−2.77	−2.74
E[b]	3.04	3.03	3.08	3.05	3.04	3.04	2.99	3.11	3.00	2.99	2.97	2.97	3.10	3.00	2.99	2.98

[a] The solvent is CH_3OH.
[b] E = LUMO–HOMO, the energy gap.

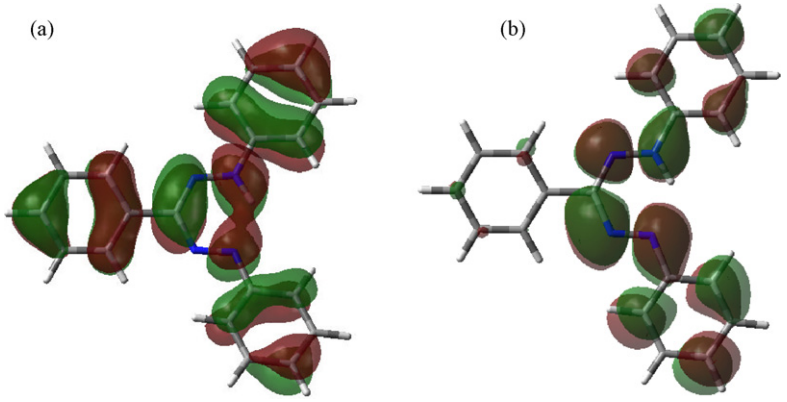

Fig. 4. The (a) HOMO and (b) LUMO of **TPF** at PCM-TD-PBE1PBE/6-311G(2d,2p)//PBE1PBE/6-311G(2d,2p) level.

electrons. This is known as "resonance" is least. That is why λ_{max} are shifted to the shorter wavelengths than other positions. The attachment to *p*-position for all substituents makes λ_{max} longer, because the Cl or Br join to the conjugation. The electron-donating ability of substituents is Br ≈ Cl > CH_3, and the sequence of λ_{max} Br ≈ Cl > CH_3, as explained in Section 3.2.

Table 7 lists the energies of the frontier orbitals of studied molecules at PCM-TD-PBE1PBE/6-311G(2d,2p)//PBE1PBE/6-311G(2d,2p) level. The sequence of excitation energy for the substituents is Br ≈ Cl < CH3 which is consistent with the sequence of λ_{max}. The calculation represented the excitation corresponding HOMO–LUMO transition with the strongest oscillator strength. It is seen that the main transition corresponds to $\pi \rightarrow \pi^*$ excitation for studied formazans. It is depicted the HOMO and the LUMO of **TPF** in Fig. 4. It can be seen from the figure that the HOMO of **TPF** is distributed at the main molecular skeleton, and the LUMO is localized in the Ph–N=N–C=N–N–Ph skeleton. The frontier orbitals of considered substituted formazans are similar to that of **TPF**.

4. Conclusions

1-Substituted (CH_3, Br, Cl) phenyl-3,5-diphenylformazans were synthesized and their UV–vis spectra were studied experimentally and theoretically. Structural stabilities of the studied formazans were effected by steric effect. When the *o*-position of 1-phenyl group has a substituent, the substituted phenyl group was out of the main skeleton plane. It was found that the deviation of 1-phenyl group of *o*-bromo formazan was greater than that of *o*-Cl and *o*-CH_3 substituted formazans. The main skeletons of all studied formazans that form the pseudo six-membered ring are nearly planar. But the phenyl group attached to C3-atom on the skeleton of formazan is out of this plane.

TD-PBE1PBE-PCM method was applied to the UV–vis spectra of formazans. 6-311G(2d,2p) basis set provided the best results. The comparisons of calculated and experimental λ_{max} values of studied compounds indicate that they are supported each other. It was observed that the energy difference between HOMO and LUMO was decreased by the electron-donating substituents, and λ_{max} of substituted compounds were longer wavelengths relative to that of unsubstituted formazans. From the view of excitation spectra, TD-DFT method will be helpful for the further study on the electronic spectra of formazans.

References

[1] A.R. Katritzky, S.A. Belyakov, D. Cheng, H.D. Durst, Sythesis 5 (1995) 577–581.
[2] J.W. Lewis, C. Sandorfy, Can. J. Chem. 61 (1983) 809–816.
[3] H. Tezcan, S. Can, R. Tezcan, Dyes Pigments 52 (2002) 121–127.
[4] G. Arnold, C. Schiele, Spectrochim. Acta 25A (1969) 685–696.
[5] A.F. Hegarty, F.L. Scott, J. Org. Chem. 32 (1967) 195.
[6] B.N. Barsoum, S.K. Khella, A.H.M. Elwaby, A.A. Abbas, Y.A. Ibrahim, Talanta 47 (1998) 1215–1222.
[7] V.C. Schiele, Berichte der Bunsengesellschaft 30 (1964) 308–318.
[8] A.M. Mattson, C.O. Jensen, R.A. Dutcher, Science 106 (1947) 294–295.
[9] J.A. Plumb, R. Milroy, S.B. Kaye, Cancer Res. 49 (1989) 4435–4440.
[10] S.A. O'Toole, B.L. Sheppard, E.P.J. McGuinness, N.C. Gleeson, M. Yoneda, J. Bonnar, Cancer Detect. Prev. 27 (2003) 47–54.
[11] D.M. Aziz, Anim. Reprod. Sci. 92 (2006) 1–8.
[12] H. Tezcan, E. Uzluk, M.L. Aksu, Electrochim. Acta 53 (2008) 5597–5607.
[13] S. Erkoc, H. Tezcan, E.D. Calisir, F. Erkoc, Int. J. Pure Appl. Chem. 1 (2006) 37–44.
[14] J.P. Perdew, A. Ruzsinszky, M. Tao, V.N. Staroverov, G.E. Scuseria, G.I. Csonka, J. Chem. Phys. 123 (2005) (article number: 062201).
[15] J. Jacquemin, E.A. Perpète, G.E. Scuseria, I. Coifini, C. Adamo, J. Chem. Theory Comput. 4 (2008) 123–135.
[16] g. Buemi, F. Zuccarello, P. Venuvanalingam, M. Ramalingam, S.S.C. Ammal, J. Chem. Soc.: Faraday Trans. 94 (1998) 3313–3319.
[17] R.A. King, B. Murrin, J. Phys. Chem. A 108 (2004) 4961–4965.
[18] M.J. Frisch, et al., Gaussian03 Revision D.01, Gaussian Inc., Wallingford, CT, 2004.
[19] J.P. Perdew, K. Burke, M. Ernzerhof, Phys. Rev. Lett. 77 (1996) 3865–3868.
[20] A.D. Becke, J. Chem. Phys. 98 (1993) 5648–5652.
[21] C. Lee, W. Yang, R.G. Parr, Phys. Rev. B 37 (1988) 785–789.
[22] M. Cossi, V. Barone, J. Chem. Phys. 115 (2001) 4708–4717.
[23] U. Yüksel, Post-Doctoral Thesis, Aegean University, İzmir, Turkey, 1981.
[24] L.J. Bellamy, The Infrared Spectra of Complex Molecules, Methuen Publ., London, 1962.
[25] D. Jacquemin, X. Assfeld, J. Preat, E.A. Perpète, Mol. Phys. 105 (2007) 325–331.